Characterization of Ionomer-Compatibilized Blend Morphology Using Synchrotron Small-Angle X-ray Scattering

Gregory C. Gemeinhardt and Robert B. Moore*

Department of Polymer Science, The University of Southern Mississippi, 118 College Dr. #10076, Hattiesburg, Mississippi 39406

Received October 1, 2004; Revised Manuscript Received January 21, 2005

ABSTRACT: Synchrotron SAXS was used to characterize the morphology of an amorphous ionomer-compatibilized polyester/polyamide blend. This technique was shown to provide very useful information regarding the size of the dispersed domains, the structure of the phase-separated morphology, and the thickness of the blend interface. Two blend series that were investigated include a binary system (polyamide/ionomer) with varying ion contents of the polyester ionomer and a ternary blend (polyamide/polyester/ionomer) with increased loading of an ionomer compatibilizer. The incorporation of ionic functionality, by varying either ion content or ionomer loading, has a significant impact on the sizes of the dispersed domains with both blend systems showing a trend toward smaller domain sizes with an increase in the concentration of ionic functionality. In addition, the 50/50 blend series indicates that the ionic incorporation also leads to a shift in the morphology to a more elongated, cocontinuous structure. While the ionic functionality does affect the domain sizes and structure, the location of the functional groups at the blend interface does not lead to an increase in the thickness or diffusivity of the interfacial region.

Introduction

The utilization of scattering experiments to investigate heterogeneous systems has been widely applied to a variety of samples ranging from semicrystalline polymers to ionomers and polymer blends. While small-angle laser light scattering (SALS) has been used mainly for the investigation of spherulite growth in polymer crystallization and microscale phase separation of polymer blends,[1−8] small-angle neutron and X-ray scattering (SANS and SAXS, respectively) techniques have proven very useful in a wide variety of applications due to their ability to probe much smaller size scales with a shorter wavelength irradiant beam. The ability of a sample to scatter an incident beam depends on differences in polarizability and refractive index for visible light scattering, electron density contrast for X-ray scattering, and the nature of the scattering nucleus for neutron scattering. For neutron scattering, isotopic labeling of deuterium for hydrogen has greatly increased the effectiveness of samples to scatter neutrons and proven quite useful for SANS.[9]

Neutron scattering techniques have been developed over the past few decades to extend the application of these experiments to various polymer systems including composites and polymer blends. Early application of SANS involved the study of chain conformations in amorphous and semicrystalline homopolymers.[10−13] However, development of scattering theory for phase-separated systems has allowed SANS techniques to be applied to the investigation of the morphology of heterogeneous polymer systems. Neutron scattering has since been applied to many studies involving blends and interpenetrating polymer networks (IPN's) for the investigation of various blend parameters such as correlation length of heterogeneous domains, radius of gyration of chains in miscible blends, and Flory−Huggins interaction parameters between blend components.[14−20]

Of particular importance to the current research is the application of SANS to the investigation of the morphology of functionalized and/or compatibilized polymer blends. The incorporation of functional groups onto one of the blend components can significantly affect the compatibility of the blend, as has been shown in recent reports.[14−16,19] For example, in blends of polystyrene with poly(styrene-*co*-4-bromostyrene), the degree of bromination has been shown to affect the miscibility of the blend; an increase in the degree of bromination results in a decrease in the interfacial width, as determined by neutron reflectivity.[15]

The effect of the incorporation of ionic functionality onto one of the blend components on morphology has also been investigated through SANS. The Debye−Bueche theory was used to describe the scattering behavior of polystyrene/sulfonated polystyrene[14] (PS/SPS) as well as polycarbonate/sulfonated poly(butylene terephthalate) (PC/SPBT) blends.[16] The PS/SPS blend was shown to be phase separated with the correlation length varying over a wide composition range, owing to a large positive interaction parameter between styrene and styrenesulfonic acid monomers. In the SPBT/PC blends, the temperature, blend composition, and degree of sulfonation were observed to have an effect on the compatibility of the blend. The blend was described to be miscible in the amorphous phase with the short-range correlation length describing the distance between the SPBT and PC chains, while the long-range correlation length gave the dimensions of the PBT crystallites present in the system.

Tucker and co-workers used SANS to investigate the morphology and thermodynamics of polyamide/lithium-sulfonated polystyrene (PA/LiSPS) blends.[19] A peak in the scattering intensity was observed and attributed to large-scale concentration fluctuations that arise because of the immiscibility between the unfunctionalized styrene segments and the polyamide. The occurrence of these concentration fluctuations decreased with increas-

* Corresponding author. E-mail RBMoore@usm.edu.

10.1021/ma0479823 CCC: $30.25
Published on Web 03/04/2005

ing sulfonation level due to the promotion of intermolecular interactions between sulfonate and amide groups. This effect was also accompanied by a decrease in the blend interaction parameter (χ) with increasing sulfonation level and increasing ionomer loading.

The compatibilization of polymer blends through the incorporation of block copolymers has also been investigated using SANS.[17,18,20] The block copolymers locate at the blend interface and serve to decrease the interfacial tension. In the SANS experiments, this is evident in a reduction in the blend interaction parameter and a widening of the blend interface with the incorporation of the block copolymer compatibilizer.[17,20] SANS experiments have also shown that a block copolymer can reduce the spinodal temperature for upper critical solution temperature (UCST) blends, broadening the composition vs temperature window in which the blend is miscible.[18,20]

While small-angle neutron scattering has been used to probe information such as the radius of gyration, correlation lengths, and Flory−Huggins interaction parameter, several literature reports have outlined the advantages of using synchrotron SAXS to calculate these important blend parameters.[21−24] The advantages of using SAXS over SANS include the elimination of isotopic labeling, and the high intensity/resolution of these experiments allows for fast data collection and dynamic examination of the phase-separation process in real time.

For example, SAXS has been used to characterize the morphology and heterogeneities that exist in several blend samples.[25−29] The blend morphology and phase separation kinetics of polystyrene/poly(chloro- or bromostyrene) have been extensively characterized using SAXS experiments.[21,23,30] The Ornstein−Zernike relationship was used in each to determine the interaction parameter and average radius of gyration for the blend. Rabeony and co-workers[22,24] have used synchrotron SAXS to calculate the Flory−Huggins interaction parameter (χ) of a blend consisting of poly(cyclohexyl acrylate) and poly(bromostyrene). The interaction parameter was found to be negative with the absolute value decreasing with temperature, indicative of a miscible blend exhibiting LCST behavior.

A one-parameter correlation function was used by Taylor-Smith and Register in a Debye−Bueche analysis of the SAXS behavior of a hydroxyl-functional polystyrene/poly(ethyl acrylate) (PS-OH/PEA) binary blend compatibilized through hydrogen bonding.[26] As the level of functionalization increased, the low-q scattering of the blend increased, indicative of a reduction in the domain sizes. Above a certain level of functionalization, the intensity began to drop due to an increase in the mixing of the blend components. For the blend series, the calculated correlation length progressively decreased as the level of functionalization increased.

Perrin and Prud'homme utilized SAXS to investigate the effect of the incorporation of a block copolymer as a compatibilizer on the thickness of the blend interfacial region.[27] The data analysis was based on deviations within the Porod region.[31,32] Incorporation of at least 5% of the block copolymer was necessary to observe an effect on the size of the dispersed domains, and the interface of the blends with copolymer incorporated was substantially thicker than for a mixture of just the homopolymers. Even though the values for interface thickness indicated a rather sharp boundary (~1.8−3.2 nm), the interface thickness increased by 33% with 10% incorporation of copolymer and 78% with 15% incorporation.

To date, scattering experiments have been used in a wide variety of ways to characterize the morphology of polymer blends and the effect of blending on the properties of the blend components. Investigations have included the effect of functional group concentration (hydroxyl groups in a PS-OH/PEA blend[26] or sulfonate groups in a SPS/PS blend[14]) on the blend correlation length and the effect of semicrystalline/ionomer blends on crystallization of a blend component and the ionomer morphology.[33−35] In the area of blend compatibilization, the research has been limited to studying the effect of block copolymers on the blend morphology and interfacial properties.[15,17,18,20,27] While two of reports, as described earlier, investigate the effect of sulfonation on binary blend morphology,[16,19] the influence of sulfonation on the phase separation behavior of polymer blends in the absence of crystallinity has not been fully investigated through SAXS experiments. This report describes the application of SAXS to a binary and ternary amorphous blend system that is compatibilized through the incorporation of functional groups capable of forming strong specific intermolecular interactions.

The utilization of a polyester ionomer as a minor component compatibilizer has been shown in previous research to have a significant effect on the phase morphology and mechanical properties of polyester/polyamide blends.[36] An increase in the ion content and/or ionomer incorporation resulted in reduced phase separated domain sizes as well as increased interphase mixing. The ionomer also enhanced the ultimate mechanical properties of the blends as a result of increased interfacial adhesion. The utilization of the polyester ionomer as a minor component compatibilizer decreased the dimensions of the dispersed phase and shifted the morphology from matrix/droplet to a cocontinuous structure at higher incorporations of the ionic functionality. The ionomer was shown to act as a compatibilizer for the polyester/polyamide blends through the presence of specific interactions between the ionomer sulfonate group/counterion and the amide linkage of the polyamide.

The present research aims to investigate the heterogeneity of blends of an amorphous polyester with an amorphous polyamide, compatibilized with a polyester ionomer, through the use of synchrotron SAXS. The morphological features of the blends are investigated using the Debye−Bueche scattering theory, employing a two-parameter correlation function, as a function of blend composition and the incorporation of ionic groups at three different ion contents onto the polyester backbone. The application of the Ornstein−Zernike relationship to this blend system is not valid since these calculations are based on the de Gennes random phase approximation, which assumes a miscible, homogeneous system to calculate the radius of gyration and Flory−Huggins interaction parameter. This report demonstrates the usefulness of synchrotron SAXS along with data analysis using the Debye−Bueche theory in the investigation of the morphology of ionomer-compatibilized blends.

Experimental Section

Materials. The amorphous polyester (PETG 6763) as well as the analogous sulfonated form of the amorphous polyester

(SPETG) were supplied by Eastman Chemical Co. The PETG is a glycol-modified amorphous polyester, and the backbone of SPETG is similar to PETG with the exception of randomly placed sulfoisophthalic acid units along the polymer chain, incorporated at 1.9, 3.0, and 5.5 mol % of the total monomer units (referred to as 1.9SPETG, etc.). The amorphous polyamide-6 (Durethan T40) was supplied by Bayer Corp.

Blend Preparation. Blend samples were prepared using a twin-screw extrusion blending processes. The polyester and polyester ionomer were dried in a vacuum oven at 65 °C for 24 h, while the polyamide was dried in a vacuum oven at 80 °C for 24 h to ensure complete drying. The pellets for each of the polymers were then dry mixed at the desired blend ratio and fed simultaneously into the extruder. Two sets of blends were prepared, the first a binary T40/SPETG blend at 75/25 and 50/50 weight ratio (for each of the ion contents: 0, 1.9, 3.0, and 5.5 mol %) and the second a ternary T40/PETG/5.5SPETG blend at $80/(20 - x)/x$ weight ratio with $x = 0$, 2, 5, and 10 wt %. The blends were extruded at 260 °C and 200 rpm on a Prism 16 mm corotating twin-screw extruder equipped with a tape die and calendar take-up rollers. The resulting films were ~0.35 mm thick.

SAXS Characterization. The SAXS experiments were performed on beamline X3A2 at the National Synchrotron Light Source at Brookhaven National Laboratory. The X-ray wavelength was 0.155 nm, and the data were acquired using image plates. A silver behanate standard was used to calibrate the q range and determine a sample-to-detector distance (SDD) of 1801 mm. The range of scattering vectors [$q = (4\pi/\lambda) \sin \theta$] detectable at this SDD was $0.061 \text{ nm}^{-1} < q < 2.2 \text{ nm}^{-1}$. Data were acquired using a 2 min exposure time on a sample that consisted of four disks punched from the center of the blend tape, sandwiched between two pieces of Kapton tape. Background scattering images were acquired under identical conditions, using the sample holder with Kapton tape in the absence of a sample. The beam intensities were measured using separate ionization chambers before and after the sample in order to account for the sample transmission factor.

Each of the scattering images was calibrated to a SDD of 1801 mm and azimuthally integrated around 360° using the POLAR software program (STAR, Inc.) to yield an $I(q)$ vs q plot. A Lupolen standard was obtained from Oak Ridge National Laboratory in order to convert the data from relative to absolute intensity. The data correction accounted for sample attenuation, background subtraction, thermal density fluctuations through Porod's law, and conversion to absolute intensity scale.

Theoretical Basis

The Debye−Bueche theory of light scattering from a heterogeneous, isotropic system[37,38] was used as the starting point to derive the relationships used to calculate the blend morphological parameters according to a previous derivation by Moritani and co-workers.[39] The intensity distribution of scattered light is given by

$$I(q) = \rho^2 \phi_a \phi_b \int_0^\infty \gamma(r) \frac{\sin(qr)}{qr} 4\pi r^2 \, dr \tag{1}$$

where ϕ_a and ϕ_b are the volume fractions of the T40 and PETG, respectively, ρ^2 is the electron density contrast parameter, q is the scattering vector, and r is the distance between scattering centers. The two-component correlation function for an isotropic, heterogeneous system, $\gamma(r)$, is given by

$$\gamma(r) = f \, e^{(-r/a_1)} + (1 - f) e^{-(r/a_2{}^2)} \tag{2}$$

where f is the fractional contribution factor of the short-range fluctuation to the correlation function, a_1 is an intradomain short-range correlation distance, and a_2 is an interdomain long-range correlation distance. Substituting the correlation function into the equation for the intensity distribution and carrying out the integration yields the following equation:

$$I(q) = K\left[\frac{2f a_1{}^3}{[1 + (qa_1)^2]^2} + (1 - f)\left(\frac{\pi^{1/2} a_2{}^3}{4}\right) e^{-(qa_2/2)^2}\right] \tag{3}$$

where K combines all of the constants ($= 4\pi\rho^2\phi_a\phi_b$).

The data were fit to eq 3 using a nonlinear regression analysis with four adjustable parameters, a_1, a_2, f, and ρ^2. The nonlinear regression was carried out using the DataFit v.8.0 software package and provided an excellent fit to the observed scattering data over the measured q range. The specific surface (S_{sp}), defined as the interfacial area between the two phases per unit volume of the system, can be calculated from eq 4 using the short-range correlation length (a_1) calculated from the two-parameter fit.

$$S_{sp} = \frac{f[4\phi_a(1 - \phi_b)]}{a_1} \tag{4}$$

As discussed previously, the introduction of a compatibilizer, in particular a block copolymer, into an immiscible blend has been shown to increase the thickness or diffusivity of the interfacial region.[27,31,32,40] After corrections for thermal density fluctuations, systematic deviations from Porod's law at high q values ($q \to \infty$) has been attributed to either the presence of a diffuse phase boundary (negative deviation) or thermal density fluctuations or mixing within the phases (positive deviation).[31,32,40] Thus, mathematical analysis of the data within this region provides a description of the thickness of the interface between the two blend components, for negative deviations, and the effect of a compatibilizer on the interface thickness. The scattering intensity after correction for thermal density fluctuations is given by[31]

$$I(q) = I_p(q) \, H^2(q) \tag{5}$$

where $I_p(q)$ obeys Porod's law ($= 2\pi(\Delta\rho)^2 S/q^4$) and $H^2(q)$ is a Guassian smoothing function for a sigmoidal-gradient model describing the interface and is given by

$$H^2(q) = \exp(-\sigma^2 q^2) \tag{6}$$

In this equation, σ is the standard deviation of the smoothing function and provides a means to calculate the thickness of the interfacial region. The standard deviation is related to the nominal interface width by $E = (\sqrt{12})\sigma$.[40] Thus, the scattering intensity can be given by the following equation:

$$I(q) = \left(\frac{2\pi(\Delta\rho)^2 S}{q^4}\right) \exp(-\sigma^2 q^2) \tag{7}$$

From this equation, a plot of $\ln[I(q)q^4]$ vs q^2 can be used to determine the standard deviation [$\sigma = (-m)^{1/2}$] and used to calculate the thickness of the interfacial region (E).

Results and Discussion

The resulting scattering curves of the binary blends after data correction are shown in Figure 1. Each of the scattering curves shows an upturn in the intensity ($I(q)$)

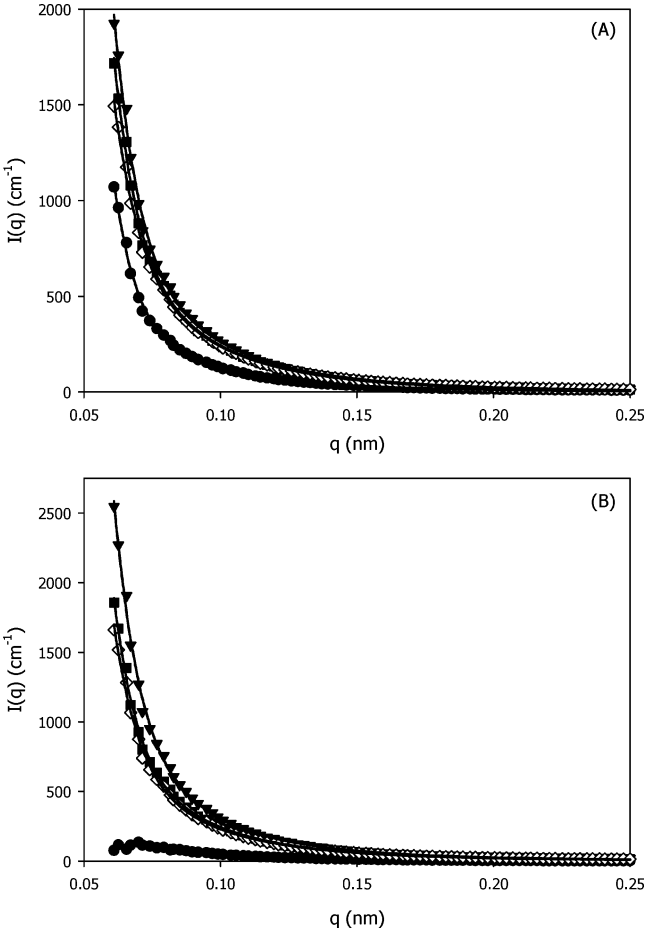

Figure 1. SAXS profiles for the polyamide/polyester binary blends having the compositions of (A) 75/25 and (B) 50/50: T40/PETG (●), T40/1.9SPETG (▼), T40/3.0SPETG (■), and T40/5.5SPETG (◆). Lines represent the fits to the data from the nonlinear regression analysis.

at small values of q, and all of the blends with ionomer show a higher intensity upturn compared to the blend with pure PETG, especially with the 50/50 blend ratio. A similar result has been observed in previous reports investigating compatibilized blends[14,26] and is indicative of a decrease in the dimensions of the dispersed phase with the incorporation of functional groups capable of forming intermolecular interactions. As the dimensions of the dispersed phase decrease, the scattering due to heterogeneity will shift to larger values of q and the intensity (maintaining a constant SDD) would be expected to increase. The scattering due to the 50/50 T40/PETG blend is minimal due to the relatively large size of the phase-separated domains. This sample has been shown through light scattering to have phase dimensions around 12 μm,[36] which is out of the range detectable using X-ray scattering at this SDD. Thus, the data analysis and calculations for the 50/50 T40/PETG blend are inaccessible and not reported here.

The lines in Figure 1 represent the nonlinear regression fits to the scattering data and show the excellent agreement between the theoretical and experimental curves. The two-parameter correlation function divides the scattering into contributions from a short-range and long-range fluctuation present in the system, and the relative contribution of each is described by the fractional contribution term, f. Figure 2 is a representative graph that illustrates the relative contribution of the two correlation lengths to the total fluctuation for the

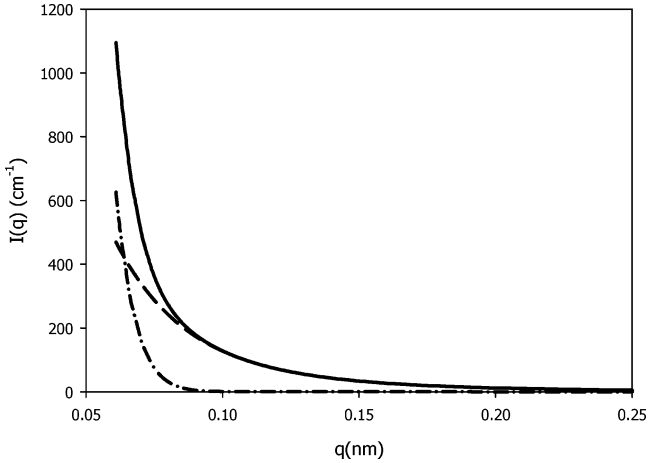

Figure 2. Relative contribution of the short-range and long-range correlation terms in the nonlinear regression analysis of the scattering for the 75/25 T40/PETG blend sample: (—) total scattering intensity, (- - -) short-range correlation, (— • —) long-range correlation.

Table 1. Morphological Parameters Determined from the Nonlinear Regression Analysis of the Scattering Data for the Binary Polyamide/Polyester Ionomer Blends

	two-parameter correlation function				
sample	a_1 (nm)	a_2 (nm)	f	S_{sp} (μm^{-1})	$\rho^2 \times 10^{-20}$ (cm^{-4})
75/25 T40/...					
PETG	17.9	66.8	0.395	15.96	2.19
1.9SPETG	17.6	63.1	0.517	21.25	3.41
3.0SPETG	18.6	64.8	0.524	20.38	3.14
5.5SPETG	17.6	61.8	0.622	25.56	2.58
50/50 T40/...					
PETG					
1.9SPETG	22.1	64.4	0.492	22.23	3.16
3.0SPETG	20.4	66.3	0.478	23.40	2.53
5.5SPETG	18.2	62.5	0.542	29.74	2.06

75/25 T40/PETG blend as described by the nonlinear regression analysis. From the figure, it can be seen that the short-range correlation term accurately describes the scattering at higher values of q while the long-range term provides a better fit to the scattering at smaller q. Combining the two terms therefore provides an excellent description of the scattering behavior of the blend samples over a wide range of q values and can be used to describe the short- and long-range correlation lengths.

The results of the nonlinear regression analysis give the morphological parameters for the binary polyamide/polyester ionomer blends, which are shown in Table 1. These data illustrate the effect of ion content on the correlation lengths and specific surface, and the electron density contrast parameter is also given for each sample. The relative contribution of the short-range correlation to the total fluctuation is accounted for by the fractional contribution factor, f. It is expected that as the domain sizes decrease, both a_1 and a_2 will decrease due to the occurrence of smaller minor phase domains (a_1) dispersed at shorter distances from each other (a_2). To accompany this, the specific surface should increase as the dimensions of the minor phase decrease.

The fractional contribution factor for all of the blends was ~0.4−0.6. This indicates that roughly 50% of the scattering intensity for the blends is attributable to the short-range correlation and is in line with values observed in other research utilizing the two-parameter correlation function.[39,41−43] The value of f increased as

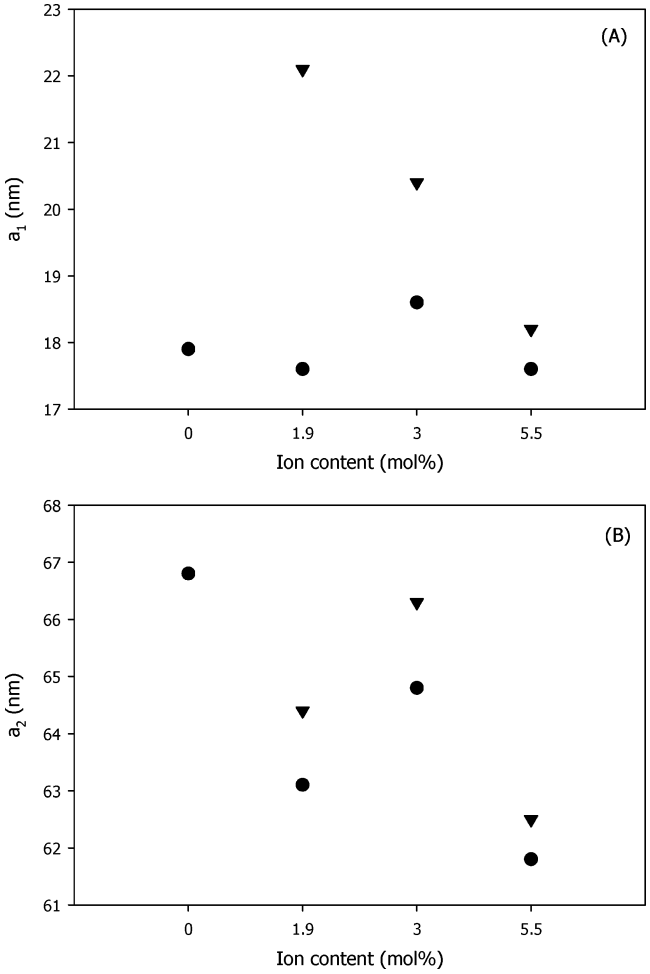

Figure 3. Correlation lengths of polyamide/polyester binary blends as a function of ion content of SPETG. (A) Short-range correlation length (a_1) and (B) long-range correlation length (a_2); 75/25 (●) and 50/50 (▼).

the long-range correlation length decreased, indicating a decrease in its contribution to the total fluctuation as the interparticle spacing decreased.

The short- and long-range correlation lengths calculated from the scattering data are shown in Figure 3. These data illustrate the effect of the ion content of the SPETG on the minor and major phase dimensions for the binary polyamide/polyester ionomer blends. As the ion content of the SPETG increases, both the short-range (Figure 3A) and long-range (Figure 3B) correlation lengths decrease, with the 50/50 blend series showing larger values compared to the 75/25 blends.

As mentioned before, the domain sizes in the 50/50 T40/PETG blends were estimated to be around 12 μm in previous research using SALS. Thus, the trend toward smaller domain sizes, both major and minor phase, with increasing ion content at a constant blend ratio indicates that the incorporation of ionic functional groups capable of forming intermolecular interactions has a significant impact on the morphology of the binary blends.

The specific surface of the binary blends is shown in Figure 4 as a function of the ion content of the SPETG in the blends. As the short-range correlation length decreases, the specific surface increases due to an increase in the surface area of the minor phase. The effect of ion content is seen in both the 75/25 and 50/50 blend series, though the 50/50 blends show a much more

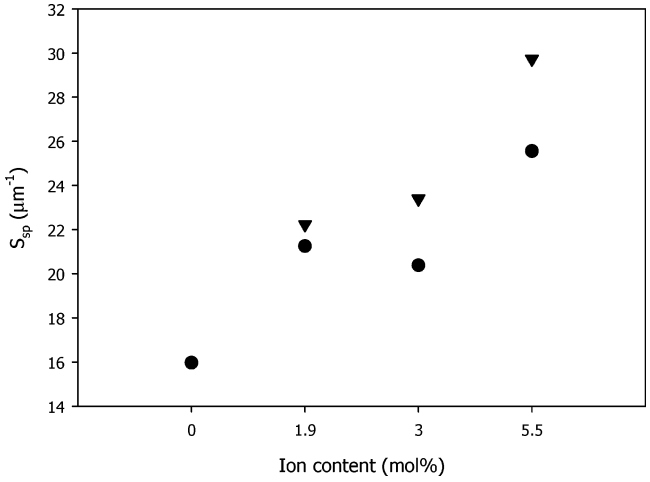

Figure 4. Specific surface of polyamide/polyester binary blends as a function of ion content of SPETG: 75/25 (●) and 50/50 (▼).

significant increase in the surface area with increasing ion content.

The relative magnitude of decrease in the values for the long-range compared to the short-range correlation length, combined with the increase in specific surface, provides an indication of the morphological structure in the binary blends. The 75/25 blend series shows a moderate reduction in both correlation lengths (1.7% for a_1 and 7.5% for a_2) with increasing ion content, indicating that the morphology is progressing toward smaller minor phase domains dispersed a shorter distance from each through the major phase. However, the 50/50 blend series shows a significant difference between the magnitude of reduction for the two correlation lengths. The short-range correlation length decreases 17.6% while the long-range correlation length decreases only 2.9% when comparing only the data for the SPETG blends. A decrease in the short-range correlation length indicates that the size of the minor phase domains is becoming smaller with increasing ion content. However, the long-range correlation length remains approximately constant with increasing ion content while the surface area of the minor phase increases dramatically. The results from the current research suggest that the minor phase is assuming a more elongated, continuous structure with increasing SPETG ion content. According to the SAXS results for the 50/50 binary blends, the short-range correlation length decreases while the surface area increases with very little effect on the long-range correlation length. These trends suggest that the minor phase is adopting a more elongated structure and indicate the onset of dual phase continuity with increasing ion content.

We have investigated the morphology of these ionomer-compatibilized T40/PETG blends in a previous report using phase-contrast optical microscopy for solution blends and environmental scanning electron microscopy (ESEM) for extruded blends.[36] The incorporation of ionomer compatibilizer resulted in a reduction in the domain sizes and a tendency to form a cocontinuous structure with increased loading of 5.5SPETG in ternary, compatibilized blends (T40/PETG/SPETG). Further research on this system, through imbedded fiber retraction, has shown that the incorporation of 5.5 mol % ionic groups onto PETG resulted in a 5-fold decrease in the interfacial tension between blend components.[44] To accompany this, the ionic functionality led

Table 2. Morphological Parameters Determined from the Nonlinear Analysis of the Scattering Data for the Ternary Polyamide/Polyester/Polyester Ionomer Blends

	two-parameter correlation function				
sample	a_1 (nm)	a_2 (nm)	f	S_{sp} (μm^{-1})	$\rho^2 \times 10^{-20}$ (cm^{-4})
T40/PETG/5.5					
80/20/0	17.9	66.0	0.401	13.68	4.41
80/18/2	18.7	67.9	0.389	12.70	4.52
80/15/5	16.4	63.6	0.439	16.35	3.67
80/10/10	15.8	61.3	0.516	19.94	4.29

to a 4−5 times increase in the lifetime of the fiber, indicating an enhanced stability of the elongated structures in the system compatibilized with ionomer. All of these results correlate extremely well with the observed trends in the SAXS data, which show a decrease in domain sizes along with a progression toward a cocontinuous network with an increase in the ion content of the ionomer.

Similar results have been observed in the scattering analysis of the morphology of IPN's.[41,45−48] An and coworkers investigated the development of the morphology in a poly(butadiene)−poly(styrene) IPN using SANS.[41] A combination of the Debye−Bueche and Guinier relationships was used to calculate the short- and long-range correlation lengths of the IPN's along with the specific surface and transverse lengths. While both correlation lengths remained nearly constant, attributed to the growth of irregular cylinders, the specific surface reached a maximum at around 50% PS content. The presence of this maximum in the surface area was attributed to the formation of a cocontinuous-type morphology. Tan and co-workers also observed a very similar trend for poly(poly(ethylene glycol) diacrylate)/epoxy IPN's.[45] As the IPN composition varied from 75/25 to 25/75, the scattering results showed a large decrease in a_1 along with only a small decrease in a_2. To accompany this, the specific surface reached a maximum at the 50/50 composition, suggesting the onset of dual phase continuity.

The results of the calculations from the nonlinear regression fits for the ternary blends (T40/PETG/5.5SPETG) are given in Table 2 and show trends that are very similar to those observed with the 75/25 binary blend series with varying ion content.

The ternary blends are based on an 80/20/0 blend ratio, varying the loading of 5.5SPETG from 2 to 10 wt %. The correlation lengths decrease accompanied by an increase in the specific surface with an increase in the loading of the 5.5SPETG ionomer. These results indicate that the ternary blends behave like a binary blend with varying ion content, as both methods of blending vary only the concentration of ionic functional groups in the blend. These functional groups serve as sites of specific intermolecular interaction that compatibilize the immiscible parent T40/PETG blend, leading to a reduction in the sizes of both the minor and major phases along with an increase in the specific surface area of the system.

The incorporation of compatibilizers, mainly block copolymers, into immiscible blends has been shown through SAXS investigations to increase the thickness or diffusivity of the interfacial region between the blend components.[27,31,32] These calculations are made by examining the deviation from linearity of the data within the Porod region and fitting the data to the equations described earlier. The results of these calculations are given in Table 3 and show the effect of ion content and ionomer loading on the thickness of the interfacial region (E).

Table 3. Standard Deviation of Gaussian Smoothing Function (σ) and Thickness of Interfacial Region (E) for Binary and Ternary Compatibilized Blends

sample	σ (nm)	E (nm)
75/25 T40/...		
PETG	0.581	2.01
1.9SPETG	0.517	1.79
3.0SPETG	0.497	1.72
5.5SPETG	0.468	1.62
50/50 T40/...		
PETG		
1.9SPETG	0.502	1.74
3.0SPETG	0.462	1.6
5.5SPETG	0.507	1.76
T40/PETG/5.5SPETG		
80/20/0	0.538	1.86
80/18/2	0.537	1.86
80/15/5	0.532	1.84
80/10/10	0.501	1.74

While the incorporation of block copolymers leads to an increase in the thickness of the blend interface, the data for the binary and ternary ionomer compatibilized blends do not show an appreciable effect of compatibilizer on the thickness of the interface. The interfacial thickness remains relatively constant regardless of the ion content (binary blends) or ionomer loading (ternary blends), and the values are similar to those observed in other immiscible blend systems with sharp interfaces.[15,27] This indicates that the location of ionic functionality along the blend interface does not significantly increase the diffusivity of the transition zone, as is the case when a block copolymer is used as the interfacial compatibilizer.

Conclusions

Synchrotron SAXS has been shown to be a very useful technique to probe the nanoscale phase-separated morphology of an amorphous ionomer-compatibilized blend. The incorporation of ionic functionality into an inherently immiscible blend, by either varying the ion content in a binary blend or increasing the ionomer loading in the ternary blend, leads to a decrease in the correlation lengths of the blend while the surface area increases. As evident in the 50/50 blends, an increase in the ion content of the SPETG additionally leads to a shift in the morphological structure. The onset of cocontinuity is reflected in the 50/50 blend series by a large reduction in the short-range correlation length with increasing ion content, accompanied by an increase in the specific surface with very little change in the long-range correlation length. As the minor phase domains adopt more elongated structures, the surface area increases with a reduction in the short-range correlation length (i.e., reflecting a relatively constant dimension of the major phase separating the minor phase domains). However, the elongated structures maintain a consistent long-range correlation length. Finally, while the location of ionic functionality at the blend interface has a significant effect on the morphology and properties of the blend, the functional groups do not significantly affect the diffusivity of the blend interface.

Acknowledgment. The authors gratefully acknowledge Eastman Chemical Co. for project funding and supplying the PETG and SPETG and Bayer Corp. for

supplying the Durethan T40. Research was carried out at the National Synchrotron Light Source, Brookhaven National Laboratory, which is supported by the U.S. Department of Energy, Division of Materials Sciences and Division of Chemical Sciences, under Contract DE-AC02-98CH10886.

References and Notes

(1) Landis, F. A.; Moore, R. B. *Macromolecules* **2000**, *33*, 6031.
(2) Kyu, T.; Yang, J. C. *Macromolecules* **1990**, *23*, 176.
(3) Kyu, T.; Yang, J. C. *Macromolecules* **1990**, *23*, 182.
(4) Kyu, T.; Lim, D. S. *J. Chem. Phys.* **1990**, *92*, 3951.
(5) Kyu, T.; Lim, D. S. *J. Chem. Phys.* **1990**, *92*, 3944.
(6) Higgins, J. S.; Guo, W. *Polymer* **1990**, *31*, 699.
(7) Prud'homme, R. E.; Perreault, F. *Polym. Eng. Sci.* **1995**, *35*, 34.
(8) Inoue, T.; Ougizawa, T. *J. Macromol. Sci., Chem.* **1989**, *A26*, 147.
(9) Higgins, J. S.; Stein, R. S. *J. Appl. Crystallogr.* **1978**, *11*, 346.
(10) Lieser, G.; Fischer, E. W.; Ibel, K. *J. Polym. Sci.* **1975**, *13*, 39.
(11) Kirste, R. G.; Kruse, W. A.; Schelten, J. *Makromol. Chem.* **1972**, *162*, 299.
(12) Wignall, G. D.; Ballard, D. G. H.; Schelten, J. *Eur. Polym. J.* **1973**, *9*, 965.
(13) Wignall, G. D.; Ballard, D. G. H.; Schelten, J. *Eur. Polym. J.* **1974**, *10*, 861.
(14) Beck Tan, N. C.; Liu, X.; Briber, R.; Peiffer, D. G. *Polymer* **1995**, *36*, 1969.
(15) Guckenbiehl, B.; Stamm, M.; Springer, T. *Physica B* **1994**, *198*, 127.
(16) Kalhoro, M. S.; Gabrys, B. J.; Zajac, W.; King, S. M.; Peiffer, D. G. *Polymer* **2001**, *42*, 1679.
(17) Schnell, R.; Stamm, M. *Physica B* **1997**, *234*−*236*, 247.
(18) Sung, L.; Nakatani, A. I.; Han, C. C.; Karim, A.; Douglas, J. F.; Satija, S. K. *Physcia B* **1998**, *241*−*243*, 1013.
(19) Tucker, R. T.; Han, C. C.; Dobrynin, A. V.; Weiss, R. A. *Macromolecules* **2003**, *36*, 4404.
(20) Voge, G.; Fosser, K.; Waldow, D.; Briber, R.; Halasa, A. *J. Polym. Sci., Polym. Phys.* **2004**, *42*, 3191.
(21) Meier, H.; Strobl, G. R. *Macromolecules* **1987**, *20*, 649.
(22) Shao, H. H.; Rabeony, M.; Liang, K. S.; Siakali-Kioufala, E.; Hadjichristidis, N. *Comput. A* **1999**, *30*, 113.
(23) Ying, Q.; Chu, B.; Wu, G.; Linliu, K.; Gao, T.; Nose, T.; Okada, M. *Macromolecules* **1993**, *26*, 5890.
(24) Rabeony, M.; Shao, H. H.; Liang, K. S.; Siakali-Kioufala, E.; Hadjichristidis, N. *Macromolecules* **1997**, *30*, 7332.
(25) VanderHart, D. L.; Campbell, G. C.; Briber, R. *Macromolecules* **1992**, *25*, 4734.
(26) Taylor-Smith, R. E.; Register, R. A. *J. Polym. Sci., Polym. Phys.* **1994**, *32*, 2105.
(27) Perrin, P.; Prud'homme, R. E. *Macromolecules* **1994**, *27*, 1852.
(28) Benson, R. S.; Lee, M. W.; Grummitt, D. W. *Nanostruct. Mater.* **1995**, *6*, 83.
(29) Ma, G. Q.; Yuan, X. B.; Sheng, J.; Bian, D. C. *J. Appl. Polym. Sci.* **2002**, *83*, 2088.
(30) Gorga, R. E.; Jablonski, E. L.; Thiyagarajan, P.; Seifert, S.; Narasimhan, B. *J. Polym. Sci., Polym. Phys.* **2002**, *40*, 255.
(31) Koberstein, J. T.; Morra, B.; Stein, R. S. *J. Appl. Crystallogr.* **1980**, *13*, 34.
(32) Ruland, W. *J. Appl. Crystallogr.* **1971**, *4*, 70.
(33) Slusarczyk, C.; Suchocka-Galas, K.; Fabia, J.; Wlochowicz, A. *J. Appl. Crystallogr.* **2003**, *36*, 698.
(34) Lu, X.; Weiss, R. A. *Macromolecules* **1993**, *26*, 3615.
(35) Kim, J. S.; Kim, H. S.; Nah, Y. H.; Eisenberg, A. *Polym. Bull. (Berlin)* **1998**, *41*, 609.
(36) Gemeinhardt, G. C.; Moore, A. A.; Moore, R. B. *Polym. Eng. Sci.* **2004**, *44*, 1721.
(37) Debye, P.; Anderson, H. R., Jr.; Brumberger, H. *J. Appl. Phys.* **1957**, *28*, 679.
(38) Debye, P.; Bueche, A. M. *J. Appl. Phys.* **1949**, *20*, 518.
(39) Moritani, M.; Inoue, T.; Motegi, M.; Kawai, H. *Macromolecules* **1970**, *3*, 433.
(40) Foster, M. D. *Crit. Rev. Anal. Chem.* **1993**, *24*, 179.
(41) An, J. H.; Fernandez, A. M.; Sperling, L. H. *Macromolecules* **1987**, *20*, 191.
(42) Vaia, R. A.; Tomlin, D. W.; Schulte, M. D.; Bunning, T. J. *Polymer* **2001**, *42*, 1055.
(43) Marr, D. W. M. *Macromolecules* **1995**, *28*, 8470.
(44) Gemeinhardt, G. C.; Moore, R. B. *Polymer*, to be submitted.
(45) Tan, S.; Zhang, D.; Zhou, E. *Polym. Int.* **1997**, *42*, 90.
(46) Sobry, R.; Rassel, Y.; Fontaine, F.; Ledent, J.; Liegeois, J. M. *J. Appl. Crystallogr.* **1991**, *24*, 692.
(47) Junker, M.; Alig, I.; Firsch, H. L.; Fleischer, G.; Schulz, M. *Macromolecules* **1997**, *30*, 2085.
(48) Song, M.; Hourston, D. J.; Schafer, F. U. *J. Appl. Polym. Sci.* **2001**, *79*, 1958.

MA0479823